THE FIELD-DEPENDENT MAGNETIC PHASES OF A UNIAXIAL TWO-SUBLATTICE ANTIFERROMAGNET OF NÉEL TYPE. II. MAGNETIZATIONS, MAGNETIC SUSCEPTIBILITIES AND PHASE TRANSITIONS

By A. Pękalski

Institute of Theoretical Physics, University of Wrocław*

(Received November 13, 1970)

The results obtained in Part I of this paper are employed here in calculating the longitudinal and transversal sublattice magnetizations and the corresponding magnetic susceptibilities for the different magnetic phases. The influence of the external magnetic field and temperature on these quantities is discussed, and a qualitative analysis of the results extrapolated to the Néel temperature is shown to lead to an unorthodox phase diagram which is found to be in agreement with recent experimental results obtained on certain uniaxial antiferromagnets.

1. *Introduction*

In Part I of this paper [1], a two-sublattice antiferromagnet of Néel type with nearest-neighbour uniaxial exchange anisotropy and external magnetic field parallel or perpendicular to the anisotropy axis has been considered. Using the non-interacting spin waves approximation the formulae for the ground state energy in each magnetic phase, the spin wave spectra, and the critical field strengths for phase transitions have been derived. In the present paper, we shall utilize the results of Part I in determining the total and sublattice magnetizations and magnetic susceptibilities for each phase, and discuss the dependence of these quantities, as well as of the (approximate) ground state energy on the strength of the applied field. Also, we examine qualitatively the influence of the temperature on the magnetization and susceptibility which, upon extrapolating the results to high temperatures leads to an unorthodox phase diagram that unexpectedly agrees fairly well with experiments on some uniaxial antiferromagnets.

2. *Thermodynamical calculations*

Let us begin with the magnetization. As the sublattice magnetization vectors lie respectively along the Oz' and Oz'' coordinate axes (see Fig. 1 of Part I), the general expression

* Address: Instytut Fizyki Teoretycznej, Uniwersytet Wrocławski, Wrocław, Cybulskiego 36, Poland.

for the magnetization in the sublattice $\{k\}$ reads

$$M_{\{k\}} \equiv \mu \left\langle \sum_k S_k^z \right\rangle \to \frac{\mu}{2} NS - \mu \sum_k \langle b_k^+ b_k \rangle$$

$$= \frac{\mu}{2} NS - \mu \sum_\lambda \sum_{s=1}^{2} \{[(u_\lambda^{2s})^2 + (v_\lambda^{2s})^2] \langle \alpha_{\lambda,s}^+ \alpha_{\lambda,s} \rangle + (v_\lambda^{2s})^2\} \tag{1}$$

due to Eqs (I. 4), (I. 5) and (I. 15), where the symbol (I. x) denotes formula x of Part I. Analogously, for the sublattice {j} we have

$$M_{\{j\}} \equiv \mu \left\langle \sum_j S_j^z \right\rangle \to -\frac{\mu}{2} NS + \mu \sum_j \langle a_j^+ a_j \rangle$$

$$= -\frac{\mu}{2} NS + \mu \sum_\lambda \sum_{s=1}^{2} \{[(u_\lambda^{1s})^2 + (v_\lambda^{1s})^2] \langle \alpha_{\lambda,s}^+ \alpha_{\lambda,s} \rangle + (v_\lambda^{1s})^2\}. \tag{2}$$

In the above formulae μ is the effective atomic magnetic moment, and

$$\langle \alpha_{\lambda,s}^+ \alpha_{\lambda,s} \rangle \equiv \bar{n}_{\lambda,s} = (e^{\beta E_{\lambda,s}} - 1)^{-1}; \quad \beta \equiv kT \ (s = 1,2) \tag{3}$$

is the average number of s-type particles (spin waves) at temperature T.

Taking into account (I. 46) we see that $M_{\{k\}} = -M_{\{j\}}$ in the phases SF, PC, P, PP, for which, therefore, we can drop the sublattice index, whereas in the AF phase this relation holds only in the ground state, *i.e.*, for $T = 0$°K ($\bar{n}_{\lambda,s} = 0$), as it follows from (I. 36).

Upon specifying the coefficients u_λ and v_λ in the formulae (1) and (2), we obtain the expressions for sublattice magnetizations in each phase. To distinguish the thermodynamical quantities in different phases, the upper indices AF, SF, PC, P, PP are introduced. Their values in the ground state shall be denoted by the lower index "0".

In the AF phase, for $K_\perp = 0$, the coefficients u_λ and v_λ are given by (I. 27). Hence,

$$M_{\{k\}}^{AF} = \frac{\mu}{2} NS - \frac{\mu}{2} \sum_\lambda \sum_{s=1}^{2} \{[Q_\lambda + (-1)^s] \bar{n}_{\lambda,s} + Q_\lambda - 1\},$$

$$M_{\{j\}}^{AF} = -\frac{\mu}{2} NS + \frac{\mu}{2} \sum_\lambda \sum_{s=1}^{2} \{[Q_\lambda - (-1)^s]\, n_{\lambda,s} + Q_\lambda - 1\}, \tag{4}$$

where

$$Q_\lambda \equiv \frac{\tilde{K}_{||} + 1}{\sqrt{(\tilde{K}_{||} + 1)^2 - y_\lambda^2}} \tag{5}$$

and the total magnetization $\mathcal{M}$ of the crystal in the AF phase for $K_\perp = 0$ is given by the well-known formula

$$\mathcal{M}^{AF} = M_{\{j\}}^{AF} + M_{\{k\}}^{AF} = \mu \langle \sum_j S_i^z \rangle + \mu \langle \sum_k S_k^z \rangle = \mu \sum_\lambda (\bar{n}_{\lambda,1} - \bar{n}_{\lambda,2}). \tag{6}$$

For the sublattice magnetization in the ground state we have

$$M_0^{AF} = \frac{\mu}{2} NS - \frac{\mu}{4} Nd, \qquad d \equiv \frac{2}{N} \sum_\lambda (Q_\lambda - 1) \tag{7}$$

which coincides with the result given by Keffer [2].

In the SF phase the coefficients u_λ and v_λ are given by (I. 46) and (I. 39), and the sublattice magnetization reads

$$M^{SF} = \frac{\mu}{2} NS + \frac{\mu}{4} N - \frac{\mu}{2} JS\gamma_0 \sum_\lambda \sum_{s=1}^{2} \frac{\tilde{K}_\perp + 1 - 1/2(-1)^s \gamma_\lambda (\tilde{K}_{||} - \tilde{h}^2/A)}{E_{\lambda,s}} (\bar{n}_{\lambda,s} + 1/2). \tag{8}$$

Its transversal $M_\perp^{SF}$ and longitudinal $M_{||}^{SF}$ components are

$$M_{||}^{SF} = M^{SF} \sin\varphi = M^{SF} \cdot \frac{\tilde{h}}{A}; \qquad M_\perp^{SF} = M^{SF} \cos\varphi = M^{SF} \sqrt{1 - \tilde{h}^2/A^2} \tag{9}$$

which follow directly from Fig. 1 of [1] and Eq. (I. 44), as the external magnetic field in this phase is directed along the Ox coordinate axis. The total magnetization $\mathcal{M}^{SF}$ of the crystal in the SF phase points in the direction of the field and is equal to $2M_{||}^{SF}$.

In the P phase the sublattice magnetization vectors are directed along the external field and, using the formulae (I. 46) and (I. 52) we may write them as

$$M^P = \frac{\mu}{2} NS + \frac{\mu}{4} N - \frac{\mu}{2} JS\gamma_0 \sum_\lambda \sum_{s=1}^{2} \frac{\tilde{h} - \tilde{K}_{||} - 1 - (-1)^s 1/2 \gamma_\lambda (\tilde{K}_\perp + 2)}{E_{\lambda,s}} (\bar{n}_{\lambda,s} + 1/2). \tag{10}$$

In this way we have derived the expressions for the magnetization in each phase. By differentiating these formulae with respect to the external field we obtain the expressions for the respective magnetic susceptibilities. Thus, in the AF phase (if $K_\perp = 0$) we have

$$\chi_{\{j\}}^{AF} \equiv \mu \frac{\partial M_{\{j\}}^{AF}}{\partial h} = \frac{\mu^2}{2} \beta \sum_\lambda \sum_{s=1}^{2} [1 - (-1)^s Q_\lambda] (\bar{n}_{\lambda,s} + \bar{n}_{\lambda,s}^2),$$

$$\chi_{\{k\}}^{AF} \equiv \mu \frac{\partial M_{\{k\}}^{AF}}{\partial h} = -\frac{\mu^2}{2} \beta \sum_\lambda \sum_{s=1}^{2} [1 + (-1)^s Q_\lambda] (\bar{n}_{\lambda,s} + \bar{n}_{\lambda,s}^2), \tag{11}$$

and in the SF phase (for $K_{||} \geq 0$, $K_\perp \geq 0$)

$$\chi^{SF} \equiv \mu \frac{\partial M^{SF}}{\partial h} = \mu^2 \frac{\tilde{h}}{A} \sum_\lambda \sum_{s=1}^{2} \Bigg\{ \frac{1}{4} \frac{\gamma_\lambda^2 (\tilde{K}_{||} + 2 - \tilde{h}^2/A)}{E_{\lambda,s} [\tilde{K}_\perp + 1 - (-1)^s \gamma_\lambda (\tilde{K}_{||} + 1 - \tilde{h}^2/A)]} \times$$

$$\times \left(\bar{n}_{\lambda,s} + \frac{1}{2}\right) + (-1)^s \frac{\gamma_\lambda}{2} \beta \frac{\tilde{K}_\perp + 1 - (-1)^s 1/2 \gamma_\lambda (\tilde{K}_{||} - \tilde{h}^2/A)}{\tilde{K}_\perp + 1 - (-1)^s \gamma_\lambda (\tilde{K}_{||} + 1 - \tilde{h}^2/A)} (\bar{n}_{\lambda,s} + \bar{n}_{\lambda,s}^2) \Bigg\}. \tag{12}$$

In the latter case, we obtain for the longitudinal susceptibility

$$\chi_{\|}^{SF} \equiv \mu \frac{\partial M_{\|}^{SF}}{\partial h} = \frac{1}{A}\left[\chi^{SF}\tilde{h} + \frac{\mu}{JS\gamma_0} M^{SF}\right]. \tag{13}$$

In the P phase (for $K_{\perp} \geqslant 0$, $K_{\|} \geqslant 0$) we get

$$\chi^{P} \equiv \mu \frac{\partial M^{P}}{\partial h} = \frac{\mu^2}{8}\tilde{K}_{\perp}(JS\gamma_0)^2 \sum_{\lambda}\sum_{s=1}^{2} \frac{y_{\lambda}^2}{(E_{\lambda,s})^3}\left(\bar{n}_{\lambda,s} + \frac{1}{2}\right) +$$

$$+ \frac{\mu^2}{2}\beta(JS\gamma_0)^2 \sum_{\lambda}\sum_{s=1}^{2}\left(\frac{\tilde{h} - \tilde{K}_{\|} - 1 + (-1)^s 1/2\, y_{\lambda}(\tilde{K}_{\perp}+2)}{E_{\lambda,s}}\right)^2 (\bar{n}_{\lambda,s} + \bar{n}_{\lambda,s}^2). \tag{14}$$

Using the formulae (4) — (14) we are able now to determine the magnetization and susceptibility in the ground state ($T = 0$°K) for the critical values of the external field. In the AF phase the zero-temperature magnetization does not depend on the field. In the SF phase, we obtain upon substituting the lower critical field (I. 50) into (8)

$$M_0^{SF}|_{\tilde{h}_{c_1}} = \frac{\mu N}{4}(2S - c_1) \tag{15}$$

where c_1 is a constant depending on the lattice type and on the anisotropy perpendicular ($K_{\perp}$) to the field:

$$c_1 \equiv \frac{2}{N}\sum_{\lambda} \frac{\tilde{K}_{\perp} + 1 + 1/2\, y_{\lambda}\tilde{K}_{\perp}}{\sqrt{(\tilde{K}_{\perp}+1)\,[(\tilde{K}_{\perp}+1) + \tilde{K}_{\perp} y_{\lambda} - y_{\lambda}^2]}}. \tag{16}$$

For $K_{\perp} = 0$, Eq. (15) reduces to

$$M_0^{SF}|_{\tilde{h}_{c_1}, K_{\perp}=0} = \frac{\mu N}{4}(2S - c'), \qquad c' \equiv \frac{2}{N}\sum_{\lambda}\left(\frac{1}{\sqrt{1 - y_{\lambda}^2}} - 1\right) \tag{17}$$

where the constant c' was calculated for the s.c. and b.c.c. lattices by Anderson [3] and Kubo [4]. The upper critical field (I. 50) for the SF phase gives, according to (8),

$$M_0^{SF}|_{\tilde{h}_{c_2}} = \frac{\mu N}{4}(2S - c_2) \tag{18}$$

where

$$c_2 \equiv \frac{2}{N}\sum_{\lambda}\left(\frac{\tilde{K}_{\perp} + 1 + 1/2\, y_{\lambda}(\tilde{K}_{\perp}+2)}{\sqrt{(\tilde{K}_{\perp}+1)\,[(\tilde{K}_{\perp}+1) + y_{\lambda}(\tilde{K}_{\perp}+2) + y_{\lambda}^2]}} - 1\right) \tag{19}$$

is another constant depending on the lattice type and anisotropy $K_{\perp}$. For $K_{\perp} \doteq 0$ we have $c_2 = 0$, and (18) reduces to the well-known result [5]

$$M_0^{SF}|_{\tilde{h}_{c_2}, K_{\perp}=0} = \frac{\mu}{2} NS. \tag{20}$$

In the P phase the insertion of the critical field (I. 58) into (10) yields

$$M_0^P|_{\tilde{h}_{c_2}} = \frac{\mu N}{4}(2S - c_2) \tag{21}$$

which is identical with (18).

Similarly, we can determine the susceptibilities for the critical field strengths in the ground state. As is seen from (11) in the AF phase we have for $T = 0°K$, regardless of the field strength,

$$\chi_0^{AF} = 0. \tag{22}$$

For the lower critical field (I. 50) in the SF phase, we have from (12)

$$\chi_0^{SF}|_{\tilde{h}_{c_1}} = \frac{\mu^2 N}{16 J S \gamma_0}\left(\frac{\tilde{K}_{||} - \tilde{K}_{\perp}}{A}\right)^{1/2} \frac{\tilde{K}_{\perp}+2}{\tilde{K}_{\perp}+1} c_3, \tag{23}$$

where

$$c^3 \equiv \frac{2}{N}\sum_{\lambda} \frac{y_\lambda^2}{1-y_\lambda^2} \frac{1}{\sqrt{(\tilde{K}_{\perp}+1)[(\tilde{K}_{\perp}+1)+\tilde{K}_{\perp} y_\lambda - y_\lambda^2]}}. \tag{24}$$

For $K = 0$, Eq. (23) reduces to

$$\chi_0^{SF}|_{\tilde{h}_{c_1}, K_{\perp}=0} = \frac{\mu^2 N}{4 J S \gamma_0}\left(\frac{\tilde{K}_{||}}{\tilde{K}_{||}+2}\right)^{1/2} c_4, \tag{25}$$

where

$$c_4 \equiv \frac{2}{N}\sum_{\lambda} \frac{y_\lambda^2}{(1-y_\lambda^2)^{3/2}}. \tag{26}$$

Substituting the upper critical field for the SF phase in (12) we have

$$\chi_0^{SF}|_{\tilde{h}_{c_2}} = \frac{\mu^2 N}{8 J S \gamma_0} \frac{\tilde{K}_{\perp}}{\tilde{K}_{\perp}+1} c_5, \tag{27}$$

where c_5 is still another constant depending on the crystal type:

$$c_5 \equiv \frac{2}{N}\sum_{\lambda} \frac{y_\lambda^2}{1+y_\lambda} \frac{1}{\sqrt{(\tilde{K}_{\perp}+1)\,[(\tilde{K}_{\perp}+1)+y_\lambda(\tilde{K}_{\perp}+2)+y_\lambda^2]}}. \tag{28}$$

For $K_{\perp} = 0$ we have $\chi_0^{SF}|_{\tilde{h}_{c_2}, K_{\perp}=0} = 0$, as is readily seen from (27). To obtain the respective expressions for the longitudinal susceptibility $\chi_{||}^{SF}$ one has to use Eqs (13), (I. 50), (23) — (28) and (15) — (20). In the P phase we get from Eq. (14) for the critical field (I. 58) and $T = 0°K$

$$\chi_0^P|_{\tilde{h}_{c_2}} = \frac{\mu^2 N}{16 J S \gamma_0} K_{\perp} c_6, \tag{29}$$

where

$$c_6 \equiv \frac{2}{N} \sum_\lambda \frac{y_\lambda^2}{\{(\tilde{K}_\perp+1)[(\tilde{K}_\perp+1)+y_\lambda(\tilde{K}_\perp+2)+y_\lambda^2]\}^{3/2}}. \tag{30}$$

Like in the *SF* phase the susceptibility (29) vanishes if $K_\perp = 0$.

3. The approximate ground state energy as a function of the external magnetic field

The ground state energy is given in the *AF* phase by Eq. (I. 37), in the *SF* phase by Eq. (I. 48), for the *PC* phase by (I. 59), and for the *P* and *PP* phases by (I. 59). As the expression for the approximate ground state energy E_0 in the *AF* phase is for $K_\perp \neq 0$ rather complicated (see (I. 22) and Appendix in Part I), we limit the discussion of the ground state energy to the case when there is a single magnetically preferred direction (*i.e.*, $K_\perp = 0$ for the *AF*, *SF*, *P* phases and $K_{||} = 0$ for the *PF* case). Taking into account that in the *SF*, *PC*, *P*, *PP* phases we have $\sum_\lambda E_{\lambda,1} = \sum_\lambda E_{\lambda,2}$, the energies in the particular phases have the following form: in the *AF* phase

$$E_0^{AF} = -\tfrac{1}{2} JNS\gamma_0\{(\tilde{K}_{||}+1)S+d_1\}, \tag{31}$$

where

$$d_1 \equiv (\tilde{K}_{||}+1)\frac{2}{N}\sum_\lambda \left(1-\sqrt{1-\frac{y_\lambda^2}{(\tilde{K}_{||}+1)^2}}\right), \tag{32}$$

in the *SF* phase

$$E_0^{SF} = -\frac{1}{2} JNS\gamma_0\left(S+1+S\frac{\tilde{h}^2}{\tilde{K}_{||}+2}\right)+$$
$$+JS\gamma_0\sum_\lambda\sqrt{\left[1+\frac{1}{2}y_\lambda\left(\frac{\tilde{h}^2}{\tilde{K}_{||}+2}-\tilde{K}_{||}\right)\right]^2-\frac{1}{4}y_\lambda^2\left(\tilde{K}_{||}+2-\frac{\tilde{h}^2}{\tilde{K}_{||}+2}\right)^2}, \tag{33}$$

in the *PC* phase

$$E_0^{PC} = -\frac{1}{2} JNS\gamma_0\left\{S(\tilde{K}_\perp+1)+\frac{\tilde{h}^2}{\tilde{K}_\perp+2}\right)+(\tilde{K}_\perp+1)\Big\}+$$
$$+JS\gamma_0\sum_\lambda\sqrt{\left[\tilde{K}_\perp+1+\frac{1}{2}y_\lambda\frac{\tilde{h}^2}{\tilde{K}_\perp+2}\right]^2-\frac{1}{4}y_\lambda^2\left(2-\frac{\tilde{h}^2}{\tilde{K}_\perp+2}\right)^2}, \tag{34}$$

in the *P* phase

$$E_0^P = -1/2\ JNS^2\gamma_0(2\tilde{h}-\tilde{K}_{||}-1), \tag{35}$$

and in the *PP* phase

$$E_0^{PP} = -1/2\ JNS\gamma_0\{S(2\tilde{h}-1)+(\tilde{h}-1)\}+$$
$$+JS\gamma_0\sum_\lambda\sqrt{[\tilde{h}-1+1/2y_\lambda(\tilde{K}_\perp+2)]^2-1/4y_\lambda^2K_\perp^2}. \tag{36}$$

From the formulae (31) — (36) we can easily get the values of the approximate ground state energies for the critical fields. As follows from (31), E_0^{AF} does not depend on the field, and for $\tilde{h}=\tilde{h}_{c_1}$ retains the value given by (31). In the SF phase (if $K_\perp=0$), upon inserting the lower critical field $\tilde{h}=\tilde{h}_{c_1}=\sqrt{\tilde{K}_{||}(\tilde{K}_{||}+2)}$ into Eq. (33) we get

$$E_0^{SF}=-\tfrac{1}{2}\,JNS\gamma_0\{S(\tilde{K}_{||}+1)+c\}, \tag{37}$$

where the constant $c\equiv\dfrac{2}{N}\sum\limits_{\lambda}(1-\sqrt{1-y_\lambda^2})$ was calculated for the s.c. and b.c.c. lattices in [3] and [4].

Assuming now the anisotropy constant $K_\perp$ in the PC phase to be equal to the anisotropy constant $K_{||}$ in the SF phase (for the sake of comparison), and taking for the field $\tilde{h}$ in the PC phase the critical value $\tilde{h}_{c_1}$ of the SF phase, we get from (34)

$$E_0^{PC}=-\frac{1}{2}\,JNS\gamma_0\left\{S(2\tilde{K}_\perp+1)+\frac{(2-\tilde{K}_\perp)^2}{8(\tilde{K}_\perp+1)}\,\frac{2}{N}\sum_\lambda y_\lambda^2+\sum_\lambda \mathcal{O}(y_\lambda^4)\right\}, \tag{38}$$

when noting that $|y_\lambda|\leqslant 1$.

For the upper critical field $\tilde{h}=\tilde{h}_{c_2}=\tilde{K}_{||}+2$ in the SF phase, we get from (33)

$$E_0^{SF}=-1/2\,JNS^2\gamma_0(\tilde{K}_{||}+3), \tag{39}$$

and for the PC phase, when $\tilde{h}_{c_2}=\tilde{K}_\perp+2$,

$$\begin{aligned}E_0^{PC}&=-\frac{1}{2}\,JNS\gamma_0\left\{(2\tilde{K}_\perp+3)S+(\tilde{K}_\perp+1)+JS\gamma_0\sum_\lambda\sqrt{(\tilde{K}_\perp+1+y_\lambda)^2+y_\lambda\tilde{K}_\perp(\tilde{K}_\perp+1+y_\lambda)}\right.\\&=-\frac{1}{2}\,JNS^2\gamma_0(2\tilde{K}_\perp+3)-\frac{1}{8}\,JS\gamma_0\tilde{K}_\perp^2\sum_\lambda\frac{y_\lambda^2}{(K_\perp+1)^2-y_\lambda^2}-\sum_\lambda\mathcal{O}(y_\lambda^4).\end{aligned} \tag{40}$$

Putting $\tilde{h}=\tilde{h}_{c_2}=\tilde{K}_{||}+2$ in (35) we get for the P phase

$$E_0^{P}=-\tfrac{1}{2}\,JNS^2\gamma_0(\tilde{K}_{||}+3), \tag{41}$$

whereas for the PP phase ($\tilde{h}_{c_2}=\tilde{K}_\perp+2$) we have

$$\begin{aligned}E_0^{PP}&=-\frac{1}{2}\,JNS\gamma_0\left\{(2\tilde{K}_\perp+3)S+(\tilde{K}_\perp+1)+JS\gamma_0\sum_\lambda\sqrt{(\tilde{K}_\perp+1+y_\lambda)^2+y_\lambda\tilde{K}_\perp(\tilde{K}_\perp+1+y_\lambda)}\right.\\&=-\frac{1}{2}\,JNS^2\gamma_0(2\tilde{K}_\perp+3)-\frac{1}{8}\,JS\gamma_0\tilde{K}_\perp^2\sum_\lambda\frac{y_\lambda^2}{(\tilde{K}_\perp+1)^2-y_\lambda^2}-\sum_\lambda\mathcal{O}(y_\lambda^4).\end{aligned} \tag{42}$$

Comparing now Eqs (31) and (37), and taking into account that $c\geqslant d_1$ (the equality sign holds only if $K_\perp=K_{||}=0$), we see that for the first (lower) critical field we have

$$\lim_{\tilde{h}\to\tilde{h}_{c1}-0} E_0^{AF}>\lim_{\tilde{h}\to\tilde{h}_{c1}+0} E_0^{SF}, \tag{43}$$

and for the PC phase, if $K_{||}$ in the AF phase is equal to $K_{\perp}$ in the PC phase, we obtain

$$\lim_{\tilde{h}\to\tilde{h}_{c1}-0} E_0^{AF} > \lim_{\tilde{h}\to\tilde{h}_{c1}+0} E_0^{PC}. \tag{44}$$

The sign of the difference $(\lim_{\tilde{h}\to\tilde{h}_{c1}+0} E_0^{SF})-(\lim_{\tilde{h}\to\tilde{h}_{c1}+0} E_0^{PC})$ depends on the values of S, γ_0, $K_{\perp}$, $K_{||}$ and increases with increasing K and/or S but decreases with increasing γ_0. For an NaCl-type antiferromagnet ($\gamma_0=6$) with $S=1$, $\tilde{K}_{\perp}=\tilde{K}_{||}=0.1$ this difference is positive, but for materials with sufficiently small anisotropy ($\tilde{K}\lesssim 0.01$) it can become negative.

Examining Eqs (39) — (42) for $K_{\perp}=0$ in the SF, P phases and for $K_{||}=0$ in the PC and PP phases we get

$$\lim_{\tilde{h}\to\tilde{h}_{c2}-0} E_0^{SF} = \lim_{\tilde{h}\to\tilde{h}_{c2}+0} E_0^{P}; \quad \lim_{\tilde{h}\to\tilde{h}_{c2}-0} E_0^{PC} = \lim_{\tilde{h}\to\tilde{h}_{c2}+0} E_0^{PP}, \tag{45}$$

$$\lim_{\tilde{h}\to\infty} (E_0^{P}-E_0^{PP}) = -\tfrac{1}{2} JNS\gamma_0(1-S\tilde{K}_{||}). \tag{46}$$

Moreover, if $K_{\perp}$ in the PC phase is equal $K_{||}$ in the SF phase, we have

$$\lim_{\tilde{h}\to\tilde{h}_{c2}-0} E_0^{PC} < \lim_{\tilde{h}\to\tilde{h}_{c2}-0} E_0^{SF}. \tag{47}$$

Let us note that the difference (46) is independent of $K_{\perp}$ and negative for true antiferromagnets, as $S\tilde{K}<1$. Finally, if $K_{||}$ in the AF phase and $K_{\perp}$ in the PC phase are equal, then

$$\lim_{\tilde{h}\to 0_+} E_0^{PC} = \lim_{\tilde{h}\to 0_+} E_0^{AF}. \tag{48}$$

The above results lead to the dependence of the approximate ground state energy on the external field as shown schematically in Fig. 1.

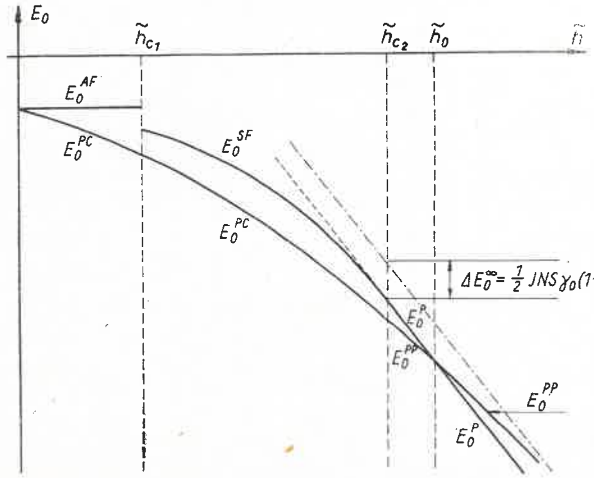

Fig. 1

4. The magnetization and susceptibility as functions of the external field and temperature

First, we shall supplement the formulae derived in Section 2 with the expressions for the total magnetization in the ground state and critical field strengths. As before, we shall restrict our considerations to the case of a single magnetically preferred direction, *i.e.*, $K_\perp = 0$ for the *AF*, *SF*, *P* phases and $K_{||} = 0$ for the *PC* and *PP* phases.

As follows from (6), in the *AF* phase the zero-temperature total magnetization $\mathcal{M}_0^{AF}$ vanishes. From Eqs (8), (9) it is seen that the total magnetization $\mathcal{M}_{SF}^0$ in the *SF* phase increases with applied field faster than linearly, from the value

$$\mathcal{M}_0^{SF}|_{\tilde{h}_{c_1}} = \frac{\mu N}{2}(2S-c')\frac{\tilde{h}_{c_1}}{A} = \frac{\mu N}{2}(2S-c')\left(\frac{\tilde{K}_{||}}{\tilde{K}_{||}+2}\right)^{1/2} \tag{49}$$

following from (9) and (17) for $\tilde{h} = \tilde{h}_{c_1}$ to the saturation value

$$\mathcal{M}_0^{SF}|_{\tilde{h}_{c_2}} = \mu NS, \tag{50}$$

which follows from (9) and (20) for $\tilde{h} = \tilde{h}_{c_2}$ and is conserved throughout the *P* phase. In the *PC* phase, the total magnetization, according to Eqs (8) and (9), also increases faster than linearly, from $\mathcal{M}_0^{PC} = 0$ for $\tilde{h} = 0$, through the value

$$\mathcal{M}_0^{PC}|_{\tilde{h}_{c_1}} = \frac{\mu N}{2}(2S-c_1)\frac{\tilde{h}_{c_1}}{A} \qquad (c_1 < c') \tag{51}$$

for $\tilde{h} = \tilde{h}_{c_1}$ following from (15), up to the value

$$\mathcal{M}_0^{PC}|_{\tilde{h}_{c_2}} = \frac{\mu N}{2}(2S-c_2) \tag{52}$$

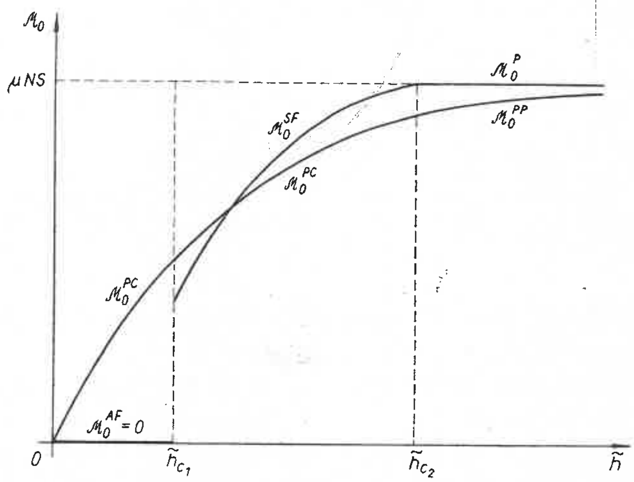

Fig. 2

for $\tilde{h} = \tilde{h}_{c_2}$, in accordance with (18). The saturation value μNS is reached not until in the *PP* phase for an infinite field, as can be easily deduced from (10) and (I. 57).

From the above results and using Eqs (7), (8), (10) for $T = 0°$K and Eqs (15) — (21)

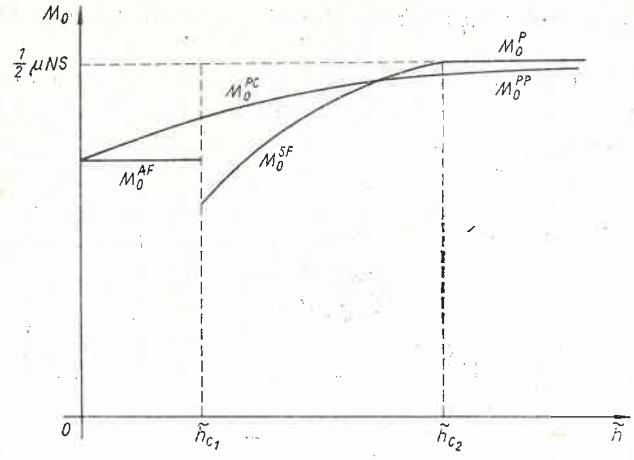

Fig. 3

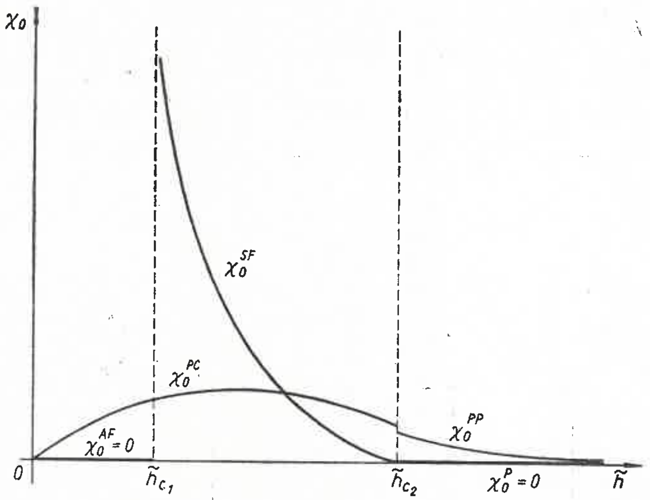

Fig. 4

we can plot the total and sublattice magnetizations in the ground state *versus* the applied magnetic field, as shown schematically in Figs 2 and 3.

The susceptibility curves $\chi_0(\tilde{h})$, corresponding to the sublattice magnetization curves of Fig. 3, can be obtained from Eqs (11), (12), (14) for $T = 0$°K, and Eqs (22) — (30). They are schematically drawn in Fig. 4.

To demonstrate, at least qualitatively, the influence of the temperature on the sublattice magnetizations and susceptibilities, schematic curves for $T \ll T_N$, based on Eqs (4), (8), (10) and Eqs (11) — (14) are shown in Figs 5 and 6 for the *AF*, *SF* and *P* phases, along with the curves corresponding to the longitudinal ($\|$) and transversal ($\perp$) components. For comparison the respective curves for $T = 0$°K are also presented in Figs 5 and 6.

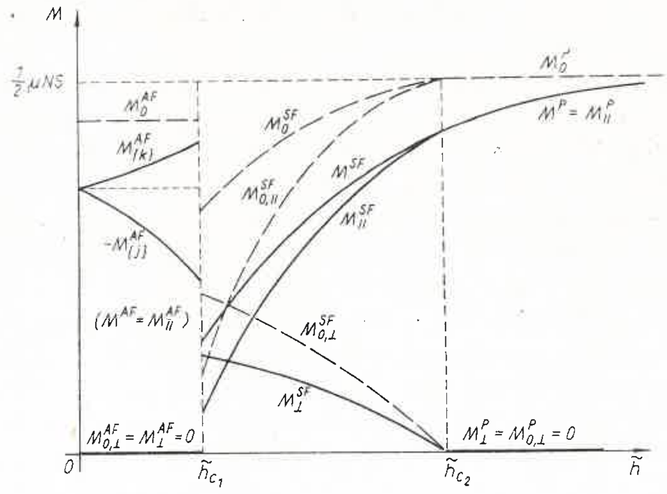

Fig. 5

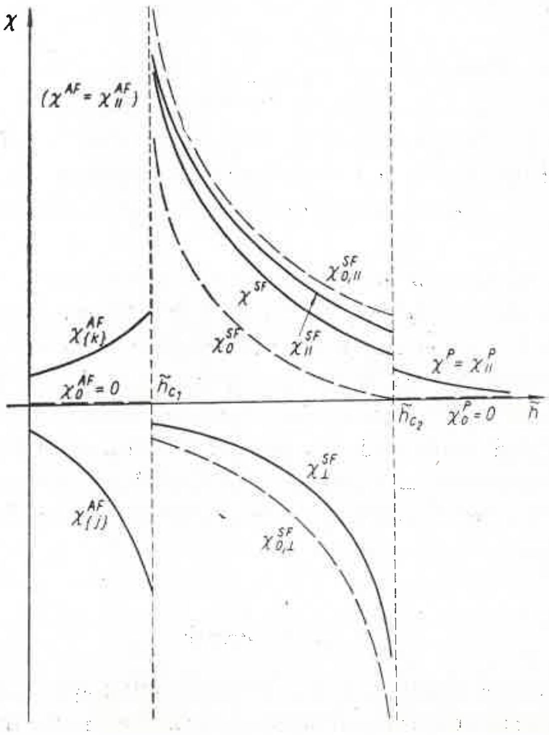

Fig. 6

5. *Discussion of the results*

Perhaps the most interesting conclusions can be drawn from analysing the energy curves of Fig. 1. Let us note that for fields $\tilde{h} \in [0, \tilde{h}_0]$ the lowest-lying is the E_0^{PC} curve and its continuation E_0^{PP}, both corresponding to the case when the field is perpendicular to the (single) anisotropy axis. For $\tilde{h} > \tilde{h}_0$, the curve E_0^{PP} lies above the straight line E_0^P and tends for $\tilde{h} \to \infty$ to an asymptote which supersedes E_0^P by $\Delta E_0^\infty = \frac{1}{2} JNS\,\gamma_0(1-S\tilde{K}_{||})$. This leads to the conclussion that in a uniaxial antiferromagnet the magnetization process occurs energetically easier for a perpendicular field. It should be noted that this fact may give rise to an interesting effect while magnetizing a uniaxial antiferromagnet in its magnetically preferred direction, provided the uniaxial magnetic anisotropy results from a spontaneous homogeneous lattice deformation due to the interactions between atomic magnetic moments. In this case, namely, the change of the spins orientation when passing from the *AF* to the *SF* phase should cause an analogous change of the anisotropy direction, and hence a transition to the *PF* case (*PC* phase). Therefore, when increasing the field the system's ground state energy would change according to the scheme $E_0^{AF} \to E_0^{PC} \to E_0^{PP}$, rather than $E_0^{AF} \to E_0^{SF} \to E_0^P$. Consequently, when switching off the field the system would regain the energy E_0^{AF} along the continuous curve E_0^{PC}, thus avoiding the discontinuity at the point $\tilde{h} = \tilde{h}_{c_1}$ (phase transition $SF \leftrightarrow AF$) and following the cycle $E_0^{AF} \to E_0^{PC} \to$ $\to E_0^{AF} \to \ldots$ In each cycle the system would at the transition $AF \to PC$ emit the energy equal to the difference $E_0^{AF} - E_0^{PC}$, as given by Eqs (31) and (38), which for $T > 0°K$ should lead to a cooling effect.

Let us also note that the curves in Fig. 1 are drawn under the assumption that $K_{||}$ in the *AF*, *SF*, *P* phases is equal to $K_\perp$ in the *PF* case. If, however, $K_{||} \neq K_\perp$ then the intersection point $\tilde{h}_0$ shifts, the critical field $\tilde{h}_{c_2}$ as given by (I. 50) is different for the $SF \to P$ and for the $PC \to PP$ transition, and, for appropriate values of the anisotropy constants, the curve E_0^{PC} can partly or even entirely lie above the E_0^{SF} curve (*cf.* remarks after Eq. (44)).

It is easy to identify the type of the phase transitions at the critical fields $\tilde{h}_{c_1}$ and h_{c_2} by utilizing Figs 2–6. As is seen from Figs 2, 3, 4 the $AF \to SF$ transition at $\tilde{h} = \tilde{h}_{c_1}$ is even for $T = 0°K$ of the first order, whereas this particular point does not correspond to any phase transition in the *PF* case. At the second (upper) critical field $\tilde{h} = \tilde{h}_{c_2}$ the $SF \to P$ as well as the $PC \to PP$ transition is of the second order because of the discontinuity of the longitudinal $\chi_{0,||}$ and transversal $\chi_{0,\perp}$ ground state susceptibility curves (see Figs 5 and 6). From these figures it is also seen that the "total" sublattice susceptibility is at the point $\tilde{h} = \tilde{h}_{c_2}$ continuous for $T = 0°K$ (χ_0 curve), and has a jump for $T > 0°K$ (χ^{SF} and χ^P curves in Fig. 6).

6. *Final remarks*

Utilizing the formulae obtained in the non-interacting spin waves approximation in Part I of this paper, we have been able to derive here expressions for the ground state energy and the total and sublattice magnetizations and susceptibilities for all the magnetic phases of a uniaxial antiferromagnet with the external field parallel or perpendicular to the anisotropy axis. These expressions when plotted as functions of the external field and temperature permit to identify easily the $AF \leftrightarrow SF$, $SF \leftrightarrow P$ and $PC \leftrightarrow PP$ phase transitions, of which the first one is of first, and the latter ones of the second order, in agreement with results obtained by other authors (see *e.g.*, Ref. [3], [7] and [9] in [1]).

While considering the case of the field perpendicular to the anisotropy axis it was found that the magnetization process is in this case energetically easier than for the field parallel to this axis (standard case considered in the literature). It was shown that this may lead to a cooling effect if the anisotropy originates in a spontaneous lattice deformation due to the magnetic coupling of the atomic spins.

Although the spin wave theory in its non-interacting approximation is generally not applicable to higher temperatures, it is interesting to extrapolate our results to the Néel temperature region. By doing so we shall be able to draw a phase diagram which appears to be in agreement with recent experimental results obtained for certain antiferromagnetic materials. For simplicity, we shall confine our considerations to the *AF*, *SF* and *P* phases only.

To obtain the *AF–P* phase boundary we require the *AF* sublattice magnetization which is antiparallel to the external field to be equal zero, *i.e.*,

$$M^{AF}_{\{j\}}(T, \tilde{h}) = 0. \tag{53}$$

The *SF–P* phase boundary is determined by the vanishing of the perpendicular component of the *SF* sublattice magnetization,

$$M^{SF}_{\perp}(T, \tilde{h}) = M^{SF}(T, \tilde{h}) = 0. \tag{54}$$

Consistently, and somewhat surprisingly, from Eq. (10) it follows that for the *P* phase the analogous condition

$$M^{P}(T, \tilde{h}) = 0 \tag{55}$$

leads also to finite temperatures for a transition of some kind in the presence of the (finite) external field.

The critical temperature T^P_2 following from Eq. (55) for $\tilde{h} = \tilde{h}_{c_2}$ coincides with the critical temperature T^{SF}_2 obtained from Eq. (54) for the same field strength. However, the critical temperatures T^{AF}_1 and T^{SF}_1 derived respectively from Eqs (53) and (54) for $\tilde{h} = \tilde{h}_{c_1}$ are in general different. To get the ordinary (zero-field) Néel temperature T_N one has to put $\tilde{h} = 0$ in Eq. (53). A more detailed analysis of Eqs (4), (8), and (10) shows that $T_N > T^{AF}_1$, $T^{SF}_1 < T^{SF}_2 = T^P_2 \equiv T_2$. To determine whether T^{SF}_1 or T^{AF}_1 is greater requires numerical calculations and specification of the crystal lattice. Assuming, *e.g.*, $T^{SF}_1 < T^{AF}_1$ we get the schematic phase diagram shown in Fig. 7. The *AF–SF* and *SF–P* boundaries are straight lines since in our (non-interacting spin waves) approximation the critical fields are temperature-independent. However, apart from this there are other discrepancies between our phase diagram and that following, *e.g.*, from the molecular field theory [6]. Namely, in the "classical" phase diagram one has $T_1^{SF} = T_1^{AF}$ which gives the well-known triple point; secondly, $T_2 = 0$; finally, there is no boundary dividing the P phase and the areas I, II, III which appear in our diagram as a formal extension of the applicability regions of Eqs (4), (8) and (10), resp., beyond the phase boundaries. There is a number of experimental results [7] pointing to a phase diagram of the type presented in Fig. 7. They confirm particularly well the shape of the *SF–P* phase boundary. Moreover, Schmidt and Friedberg [8] tried to pass from the *AF* to the *SF* phase via the paramagnetic areas I and II of our diagram, but they were unable to interprete the results. This might indicate the existence of a boundary of some kind between the areas I and II.

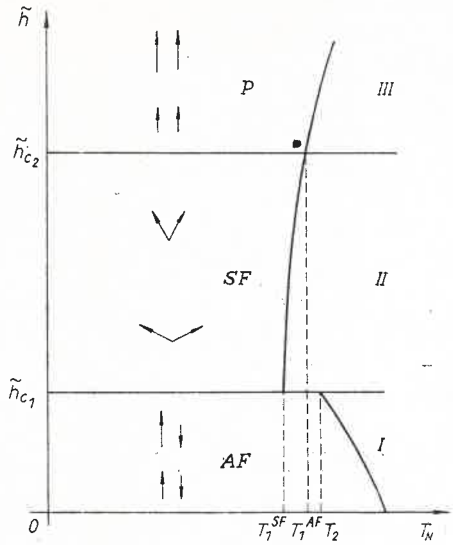

Fig. 7

There are, of course, also experiments confirming, on other antiferromagnetic materials, the "classical" phase diagram (*e.g.*, [9]). It seems, therefore, that both types of diagrams are possible — depending on the type of antiferromagnet. Should the inclusion of spin waves interactions in our considerations prove to modify for certain antiferromagnets the diagram presented in Fig. 7 into the "classical" one, then it seems reasonable to assume that in certain antiferromagnets these interactions play a significant role (are strong), whereas in others they do not. Another possible factor influencing the shape of the phase diagram might also be the type of the anisotropic magnetic coupling.

It appears, therefore, to be necessary to derive an analogous phase diagram for interacting spin waves before a decisive answer to this question can be given. Such a program is under way.

I am indebted to Dr W. J. Zietek for encouragement and many helpful comments which initiated this work, and to Mr J. M. Kowalski for valuable discussions.

REFERENCES

[1] A. Pękalski, W. J. Ziętek, *Acta Phys. Polon.*, **A39**, 327 (1971).
[2] F. Keffer, *Spin Waves* in *Handbuch der Physik*, **18/2**, Springer Verlag, Berlin-New York 1966.
[3] P. W. Anderson, *Phys. Rev.*, **86**, 694 (1952).
[4] R. Kubo, *Phys. Rev.*, **87**, 568 (1952).
[5] Y. L. Wang, H. B. Callen, *J. Phys. Chem. Solids*, **25**, 1459 (1964).
[6] C. J. Gorter, *Nuovo Cimento*, **6**, S923 (1957).
[7] W. Van der Lugt, N. J. Poulis, *Physica*, **26**, 917 (1960); H. Forstat, J. N. Elearney, P. T. Bailey, *Phys. Letters*, **27A**, 70 (1968); G. J. Butterworth, J. A. Woolam, *Phys. Letters*, **29A**, 259 (1969); G. J. Butterworth, V. S. Zidell, *J. Appl. Phys.*, **40**, 1033 (1969); J. N. Elearney, H. Forstat; P. T. Bailey, *Phys. Rev.*, **181**, 887 (1969).
[8] V. A. Schmidt, S. A. Friedberg, *J. Appl. Phys.*, **38**, 5319 (1967).
[9] H. M. Gijsman, N. J. Poulis, J. van den Handel, *Physica*, **25**, 954 (1959);
K. W. Blazey, H. Rohrer, *Phys. Rev.*, **173**, 514 (1968); H. Forstat, P. T. Bailey, J. R. Ricks, *Phys Letters*, **30A**, 52 (1969).